Published in final edited form as:
Science. 1999 November 19; 286(5444): 1566–1568.

Modulation of Respiratory Frequency by Peptidergic Input to Rhythmogenic Neurons in the PreBötzinger Complex

Paul A. Gray[1,3,*], **Jens C. Rekling**[1,*], **Christopher M. Bocchiaro**[2], and **Jack L. Feldman**[1,2,†]

[1]Department of Neurobiology, University of California Los Angeles, Box 951763, Los Angeles, CA 90095–1763, USA

[2]Department of Physiological Science, University of California Los Angeles, Box 951763, Los Angeles, CA 90095–1763, USA

[3]Interdepartmental Ph.D. Program in Neuroscience, University of California Los Angeles, Box 951763, Los Angeles, CA 90095–1763, USA

Abstract

Neurokinin-1 receptor (NK1R) and μ-opioid receptor (μOR) agonists affected respiratory rhythm when injected directly into the preBötzinger Complex (preBötC), the hypothesized site for respiratory rhythmogenesis in mammals. These effects were mediated by actions on preBötC rhythmogenic neurons. The distribution of $NK1R^+$ neurons anatomically defined the preBötC. Type 1 neurons in the preBötC, which have rhythmogenic properties, expressed both NK1Rs and μORs, whereas type 2 neurons expressed only NK1Rs. These findings suggest that the preBötC is a definable anatomic structure with unique physiological function and that a subpopulation of neurons expressing both NK1Rs and μORs generate respiratory rhythm and modulate respiratory frequency.

Respiratory rhythm is generated by neurons in the brainstem. Surprisingly, given the vital role and the apparent simplicity of breathing movements, the identity of these neurons and the mechanisms of respiratory rhythmogenesis and frequency modulation are unknown. Respiratory neurons are found in a narrow column in the ventrolateral medulla extending from the facial nucleus to the spinal cord (1,2). The preBötC is the limited portion of this column necessary and sufficient for in vitro neonatal rodent medullary slice preparations to generate respiratory-related motor nerve output (2,3). Perturbations of neuronal function within the preBötC in adult rats and cats severely disrupt breathing (4), consistent with the hypothesis that this region contains the neurons responsible for generating respiratory rhythm. Unfortunately, these and related experiments only circumscribe the approximate boundaries of the preBötC. In the absence of a precise anatomic delineation of the preBötC, defining its functional role or the roles of individual neurons it contains is problematic.

Local application of the NK1R agonist, substance P (SP), into the preBötC in vitro increases the frequency of endogenous respiratory-related output; similar application of the μOR agonist [D-Ala^2,*N*-Me-Phe^4,Gly^5-ol]enkephalin acetate (DAMGO) or the γ-aminobutyric acid type B receptor ($GABA_BR$) agonist baclofen decreases respiratory frequency (5–7). Similar responses are seen in vivo (8). Because these drugs affect frequency, they must act either directly on preBötC rhythmogenic neurons or indirectly on other preBötC neurons that provide modulatory signals to the rhythm generator. In vitro respiratory-related output does not require chlorine-mediated postsynaptic inhibition (2,3,5,9). If peptide neuromodulators affect respiratory

†To whom correspondence should be addressed. feldman@ucla.edu.
*These authors contributed equally to this work.

frequency by direct actions on only inhibitory neurons, as has been suggested for opioid actions in the midbrain (10), then peptide receptor-expressing neurons could not be responsible for rhythm generation. Thus, we examined whether the effects of SP and DAMGO on respiratory rhythm in vitro were affected by blocking GABA type A receptor ($GABA_AR$) and glycine receptor activation (11). Pressure injection of SP (2 pmol) into the preBötC of rhythmically active brainstem slices from rats increased respiratory frequency to 192% ± 5% of control, whereas injection of DAMGO (1.5 pmol) decreased frequency to 64% ± 1% of control (Fig. 1). $GABA_BR$ activation has similar effects (5,7). Bath application of the $GABA_AR$ antagonist bicuculline and the glycine receptor antagonist strychnine to these slices did not change the baseline respiratory frequency or the effects on respiratory frequency of SP or DAMGO (Fig. 1B). Thus, the preBötC NK1R-, $GABA_BR$-, and μOR-expressing neurons that mediate agonist frequency-modulating effects are likely excitatory and are either directly involved in respiratory rhythm generation or are nonrespiratory neurons that modulate rhythm-generating circuits.

We examined the immunohistochemical expression pattern of NK1R, μOR, and $GABA_BR$ in the ventrolateral medulla of adult rats (12). Within the ventrolateral respiratory column, $GABA_BR$ expression was widespread. However, both NK1R and μOR expression were concentrated within the preBötC and absent from the adjacent Bötzinger complex (BötC) (1) and rostral ventral respiratory group (1) (Fig. 2); NK1R expression in adult mouse brainstem was similar (13). The preBötC $NK1R^+$ neurons were segregated from both motoneurons and catecholaminergic sympathetic neurons as revealed by double immunohistochemistry for choline acetyl-transferase (ChAT) or tyrosine hydroxylase (TH) (13,14).

To determine whether GABAergic and peptidergic effects on breathing are due to convergent inputs onto individual neurons, we looked for μOR or $GABA_BR$ colocalization in $NK1R^+$ neurons. We found $NK1R^+/\mu OR^+$ neurons and processes (Fig. 3A) and $NK1R^+/\mu OR^-$ neurons and processes (of 88 preBötC $NK1R^+$ neurons examined in detail, 53 coexpressed μOR) (Fig. 3B). We found $NK1R^+/GABA_BR^+$ (Fig. 3C) as well as $NK1R^+/GABA_BR^-$ neurons (of 160 preBötC $NK1R^+$ neurons examined in detail, 118 coexpressed $GABA_BR$). We also found $NK1R^-/GABA_BR^+$ neurons (Fig. 3C) and a few $\mu OR^+/NK1R^-$ processes (Fig. 3B) and somas (13). Thus, GABAergic and peptidergic synaptic inputs converge on subsets of preBötC neurons. Moreover, in the ventrolateral respiratory column, neurons that are targets of these convergent modulatory inputs that affect respiratory frequency are present only in the preBötC. We propose that the expression of $NK1R^+$ neuronal somata in the ventrolateral respiratory column defines the anatomic extent of the preBötC.

These results do not differentiate whether these preBötC neurons generate or simply modulate respiratory rhythm. We tested the responsiveness of behaviorally identified respiratory neurons to neurokinin and opioid agonists (15). In the preBötC of rhythmically active slices from mice, inspiratory neurons fall into two categories (types 1 and 2) based on their electroresponsive properties and membrane potential trajectories (16,17) (Fig. 4A). After blockade of action potential driven synaptic transmission by 2 μM tetrodotoxin (TTX), bath application of SP depolarized type 1 neurons 7.7 ± 1.5 mV ($n = 4$) (Fig. 4B), whereas type 2 neurons depolarized much less [2.7 ± 0.8 mV ($n = 4$) (Fig. 4B)]. Input resistance was not significantly changed by SP in type 1 or type 2 neurons (Wilcoxon signed rank test). Bath application of DAMGO (in TTX) hyperpolarized all type 1 neurons tested (7.9 ± 1.8 mV; $n = 5$) and reduced their input resistance to 67% of control value but had no effect on either the membrane potential or input resistance of type 2 neurons ($n = 6$) (Fig. 4C). The current-voltage (*I-V*) curves of type 1 neurons before and after DAMGO (under voltage clamp in the presence of TTX) intersected at −102 mV with normal $[K^+]_o$ concentration ($n = 5$), whereas when $[K^+]_o$ was increased by 10 mM, the intersection point shifted to − 66 mV ($n = 3$; $P < 0.05$, Mann-Whitney rank sum test) (Fig.

4D). Taken together, these results suggest that the effect of DAMGO was mediated by activation of a K^+ conductance.

Most models for respiratory rhythm generation predict that depolarization of rhythm-generating neurons will speed up rhythm and that their hyperpolarization will slow it down (2,3,18). Type 1 neurons, which are rhythmogenic (2,16,17), are the only preBötC inspiratory neurons depolarized by both SP and thyrotropin-releasing hormone (16), peptides that increase respiratory frequency, and hyperpolarized by DAMGO, a peptide that decreases respiratory frequency; this is consistent with these models and the hypothesis (2) that type 1 neurons are responsible for both rhythmogenesis and frequency control.

The preBötC appears to have an important function in generating respiratory rhythm and in processing signals affecting respiratory frequency (2). We propose that the kernel for the basic respiratory rhythm is a small class of preBötC rhythmogenic neurons (type 1) onto which several modulatory systems converge. These neurons may overlap or even be identical to other preBötC neurons with intrinsic oscillatory bursting properties—for example, pacemaker neurons (3,19) and preinspiratory neurons (20)—because 50% of type 1 neurons have bursting properties (16) and at least some project to the midline (21). However, whether endogenous burst activity is critical for generation of respiratory rhythm per se (3,18–20) remains to be determined. Alterations in peptidergic transmission in the preBötC may play a role in respiratory disorders such as sleep apnea (22) and sudden infant death syndrome (23). The possibility that multiple peptide systems affecting respiration converge on a particular identifiable class of neurons represents an interesting locus for ventilatory control. The coexpression within the ventrolateral respiratory column of NK1R and μOR in preBötC neurons provides an opportunity to exploit targeted molecular manipulation of breathing in animal models and a basis for analysis of human respiratory disorders.

Acknowledgments

Supported by a Ford Foundation Pre-Doctoral Fellowship for Minorities and a predoctoral fellowship from the Porter Physiology Development Program of the American Physiological Society to P.A.G., a Parker B. Francis Fellowship to J.C.R., and NIH grants HL40959 and HL37941. We thank N. Brecha, D. Buonomono, L. Kruger, and F. Schweizer for assistance with this manuscript.

References and Notes

1. Bianchi AL, Denavit-Saubie M, Champagnat J. Physiol Rev 1995;75:1. [PubMed: 7831394] Feldman, JL. Handbooks of Physiology: The Nervous System. Intrinsic Regulatory System in the Brain. Bloom, F., editor. American Physiological Society; Bethesda, MD: 1986. p. 463-524.Dobbins EG, Feldman JL. J Comp Neurol 1994;347:64. [PubMed: 7798382]
2. Rekling JC, Feldman JL. Annu Rev Physiol 1998;60:385. [PubMed: 9558470]
3. Smith JC, Ellenberger HH, Ballanyi K, Richter DW, Feldman JL. Science 1991;254:726. [PubMed: 1683005]
4. Monnier A, Hayashi F, McCrimmon DR. Soc Neurosci Abstr 1998;346:5.Koshiya N, Guyenet PG. J Physiol London 1996;491:859. [PubMed: 8815217] Ramirez JM, Schwarzacher SW, Pierrefiche O, Olivera BM, Richter DW. J Physiol London 1998;507:895. [PubMed: 9508848] Hsieh JH, et al. J Autom Nerv Sys 1998;73:7.
5. Feldman JL, Smith JC. Ann NY Acad Sci 1989;563:114. [PubMed: 2476055]
6. Johnson SM, Smith JC, Feldman JL. J Appl Physiol 1996;80:2120. [PubMed: 8806921]
7. Brockhaus J, Ballanyi K. Eur J Neurosci 1998;10:3823. [PubMed: 9875360]
8. Bonham AC. Resp Physiol 1995;101:219.McCrimmon, DR.; Mitchell, GS. Regulation of Breathing. Dempsey, JA.; Pack, AI., editors. Vol. 79. Dekker; New York: 1995. p. 151-218.
9. Funk GD, Smith JC, Feldman JL. J Neurophysiol 1993;70:1497. [PubMed: 8283211] Shao XM, Feldman JL. J Neurophysiol 1997;77:1853. [PubMed: 9114241]

10. Fields HL, Heinricher MM. Philos Trans R Soc London Ser B 1985;308:361. [PubMed: 2858889]
11. Transverse 400- or 800-μm-thick slices of the brainstem from BALB/c mice (P_0–P_3) and Sprague-Dawley rats (P_0–P_4) were cut at the level of the caudal and rostral preBötC, respectively, as reported (3) and perfused in artificial cerebrospinal fluid (aCSF) containing 128 mM NaCl, 9 mM KCl, 0.5 mM NaH_2PO_4, 1.5 mM $CaCl_2$, 1.0 mM $MgSO_4$, 23.5 mM $NaHCO_3$, 30 mM glucose (rat), or 130 mM NaCl, 5.4 mM KCl, 0.8 mM KH_2PO_4, 26 mM $NaHCO_3$, 30 mM glucose, 1 mM $MgCl_2$, 0.8 mM $CaCl_2$ (mouse). Rhythmic respiratory-related motor output was recorded by a suction electrode placed on a XII nerve rootlet. Nerve activity was amplified, filtered at 3 Hz to 1 kHz, and rectified nerve activity was integrated. SP, DAMGO, 4,5,6,7-tetrahydroisoxazolo[5,4-*c*]pyridin3-ol (THIP) hydrochloride, glycine, and TTX were obtained from RBI and dissolved in aCSF. Drugs were microinjected with glass micropipettes (tip diameter 6 to 12 μm) lowered (100 to 300 μm) into the preBötC by micromanipulator. Injections were made with a controlled pressure source for 5 s. Ejection volume was monitored with a calibrated eyepiece reticule.
12. Female adult Sprague-Dawley rats (n = 17) and BALB/c mice (n = 2) were transcardially perfused with 4% paraformaldehyde in phosphate-buffered saline (PBS) with or without picric acid, cryoprotected in 25% sucrose PBS, embedded in OCT, sectioned at 25 to 40 μm on a cryostat, and processed free floating. Sections were incubated in primary antibody diluted in serum at 4°C for 24 to 48 hours, placed in fluorescent (Jackson Immunoresearch) or biotin (Vector Laboratories) conjugated species-specific secondary antibody overnight, and mounted on gelatin-subbed slides. In several rats, μOR immunohistochemistry was amplified with tyramine signal amplification–direct green amplification (NEN Life-sciences) and bright-field NK1R staining was visualized with a Vectastain Elite ABC kit and diaminobenzidine. Antibodies: rabbit antibody to NK1R (anti-NK1R) (1:2500 fluorescent, 1:25,000 bright field; Chemicon), guinea pig anti-$GABA_BR$ (1:3000; Chemicon), goat anti-ChAT (1:100; Chemicon), mouse anti-TH (1:1000; Boehringer Mannheim), rabbit anti-μOR (1:75,000 TSA or 1:7000 fluorescent; Instar). Bright-field images were digitally acquired (Polaroid DMC) into Photoshop (Adobe Systems) and background subtracted to remove chip nonlinearities. Confocal images were acquired with a Zeiss 410 SCM and maximal intensity projections were generated in NIH Image. All images were filtered and adjusted for contrast and light levels in Photoshop for clarity. Cell counts for coexpression were obtained by visual inspection of confocal images (n = 2).
13. Gray PA, Feldman JL. data not shown.
14. Feldman JL, Ellenberger HH. Annu Rev Physiol 1988;50:593. [PubMed: 3288108] Ellenberger HH, Feldman JL, Zhan WZ. J Comp Neurol 1990;294:212. [PubMed: 2332529] Ellenberger HH, Feldman JL. J Comp Neurol 1990;294:202. [PubMed: 2332528]
15. Neurons located at the caudal or rostral part of the preBötC in mice were visualized with differential interference contrast and infrared video microscopy. Glass micropipettes (resistances typically were 2 to 3 MW) were filled with a solution containing 115 mM $HMeSO_3$, 115 mM KOH, 5 mM NaCl, 1 mM $MgCl_2$, 0.01 mM $CaCl_2$, 0.1 mM BAPTA [1,2-bis(2-aminophenoxy)ethane-*N*,*N*,*N*′,*N*′-tetraacetic acid, tetra-K^+ salt], 10 mM Hepes, 3 mM 2-ATP(Mg^{2+}) (pH 7.3). Current- or voltage-clamp recordings were made with an Axoclamp-2A (Axon Instruments) amplifier in bridge or single electrode voltage clamp mode. The *I-V* relationship was determined by injecting a slow (7-s cycle) ramp-shaped current and plotting the rising phase of the *I-V*. Signals were recorded on videocassette (pulse code modulation; Vetter Instruments, model 3000A), digitized at 1 to 20 kHz with a Digidata 1200 A/D board (Axon Instruments) and analyzed with Axoscope software (Axon Instruments). Statistical values are given as mean ± SEM.
16. Rekling JC, Champagnat J, Denavit-Saubié M. J Neurophysiol 1996;75:811. [PubMed: 8714654]
17. Rekling JC, Champagnat J, Denavit-Saubié M. J Neurophysiol 1996;75:795. [PubMed: 8714653]
18. Butera RJ Jr, Rinzel J, Smith JC. J Neurophysiol 1999;82:382. [PubMed: 10400966] J Neurophysiol 1999;82:398. [PubMed: 10400967]
19. Koshiya N, Smith JC. Nature 1999;400:360. [PubMed: 10432113]
20. Onimaru H, Arata A, Homma I. Jpn J Physiol 1997;47:385. [PubMed: 9504127]
21. Rekling JC, Feldman JL. data not shown.
22. Fletcher, E.; Schaff, J. Abnormalities of Respiration During Sleep. Fletcher, E., editor. Grune & Stratton; Orlando, FL: 1986. p. 203-228.Fletcher EC. Cardiologia 1997;42:469. [PubMed: 9225492] Thalhofer S, Dorow P. Respiration 1997;64:2. [PubMed: 9044468]

23. Orlowski JP. Pediatrics 1986;78:233. [PubMed: 3737299] Carpentier V, Vaudry H, Mallet E, Laquerriére A, Leroux P. Neuroscience 1998;86:159. [PubMed: 9692751] Coquerel A, et al. Neurochem Int 1992;20:97. [PubMed: 1304324]

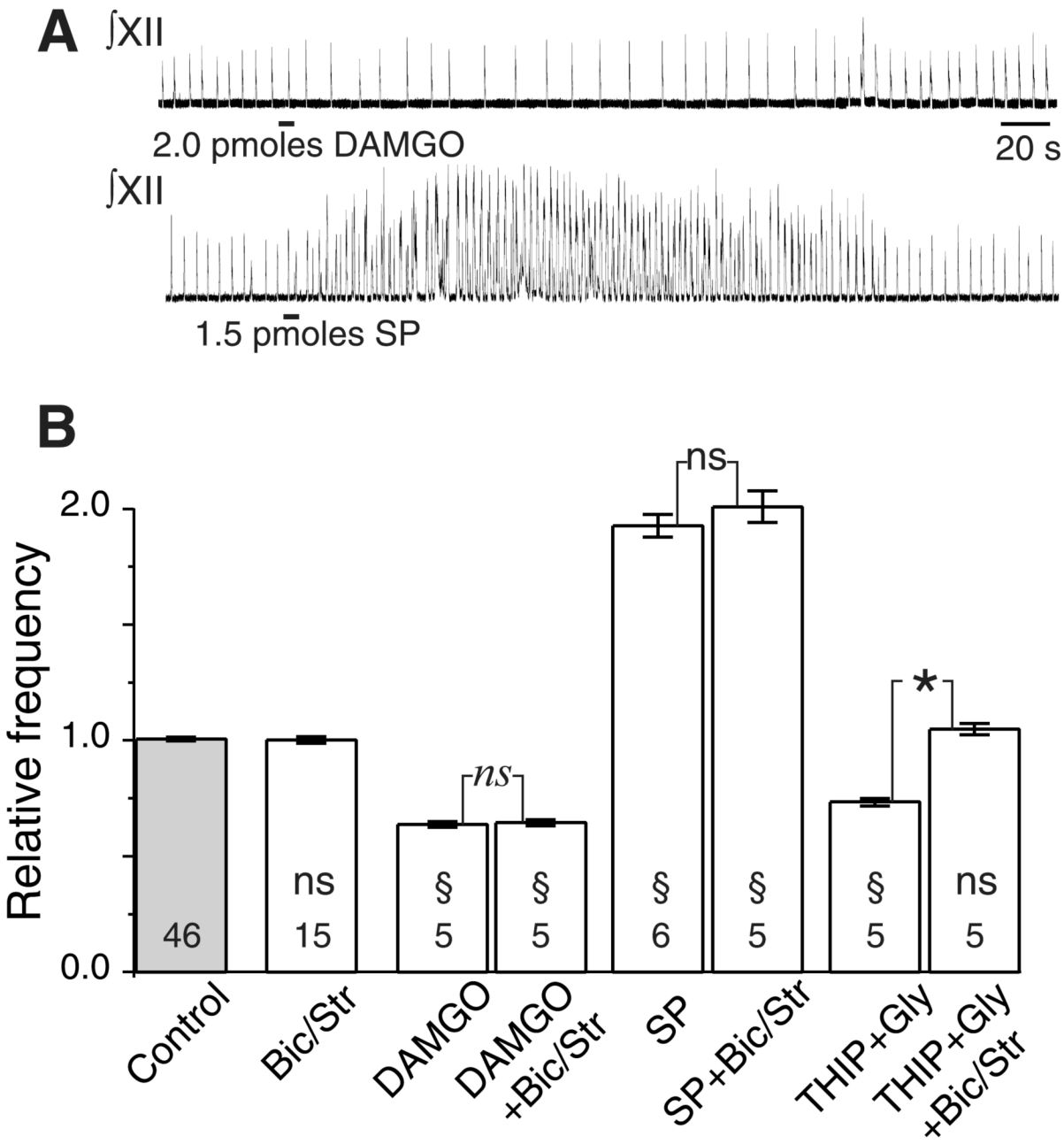

Fig. 1.

Effects of peptides injected into preBötC are independent of $GABA_A$ and glycinergic transmission. (**A**) Microinjection into preBötC of DAMGO (2 pmol) slows and SP (1.5 pmol) speeds up endogenous respiratory-related rhythm. Traces are integrated XII motor nerve output; bars under each trace represent injection period with total amount indicated. (**B**) Frequency response to microinjection of DAMGO and SP into preBötC is not affected by blocking chlorine-mediated postsynaptic transmission with bath application of bicuculline (20 μM) and strychnine (1 μM) sufficient to block the effects of the combined microinjection of the $GABA_A$ agonist, THIP (1 nmol), and glycine (1 nmol). Histograms of grouped data across multiple experiments are shown; number of epochs (20 cycles per epoch) are indicated within bars; error bars are SEM. Statistical comparisons are between individual pairs of epochs in the

same experiment: *, significant difference ($P < 0.05$; Student's *t* test) between conditions in all pairs; ns, no significant difference between conditions in all pairs; §, significant difference ($P < 0.05$) relative to control in all pairs; *ns*, no significant difference relative to control in all pairs. Bic/Str, bath application of bicuculline and strychnine.

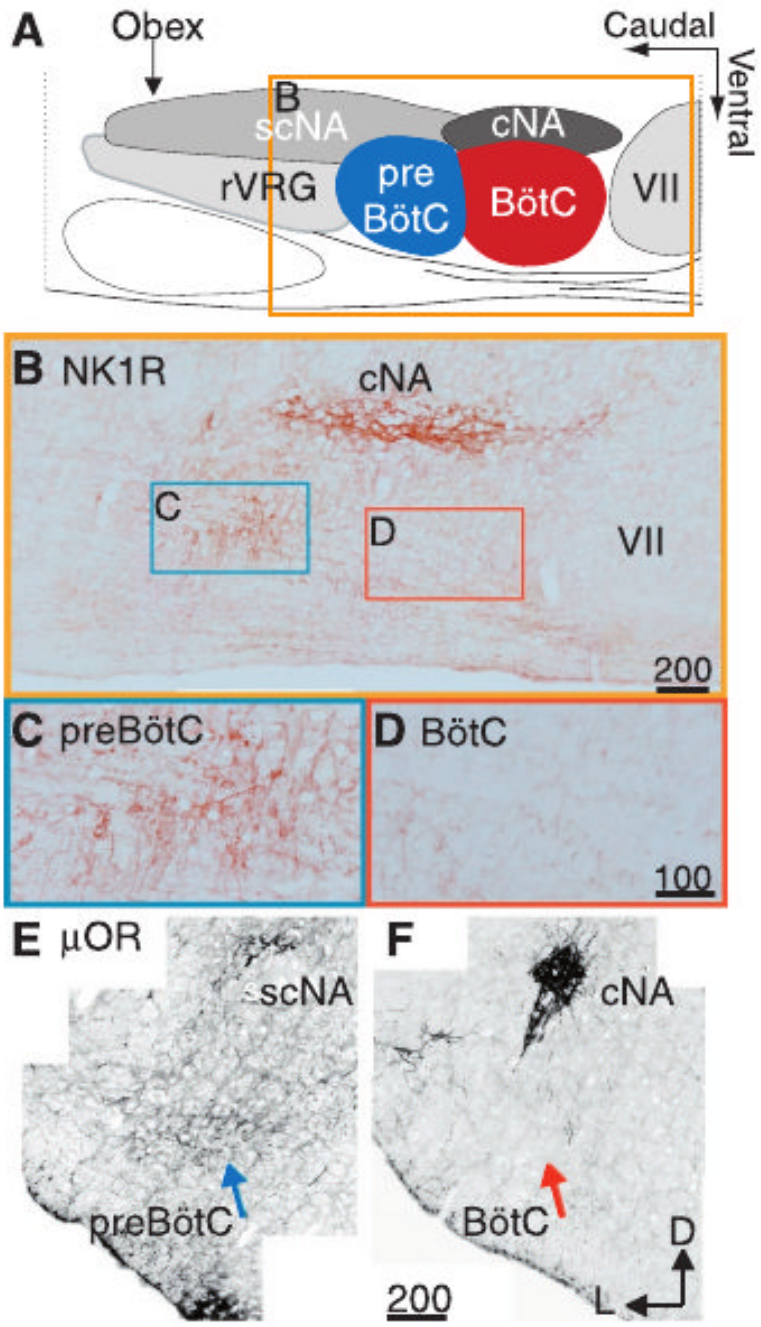

Fig. 2.

NK1R- and μOR-expressing neurons are limited to and define the preBötC. (**A**) Cartoon indicating approximate location and boundaries of ventral respiratory column regions and adjacent ambiguual motoneuron pools in sagittal section. (**B**) NK1R immunohistochemical expression in a single sagittal section through the respiratory column corresponding to box in (A). Higher magnification images showing cell soma staining from preBötC (**C**) and relative lack of staining in BötC (**D**). Confocal, negative composite images of μOR immunohistochemical staining indicating different expression levels in the preBötC (**E**) (blue arrow) and BötC (**F**) (red arrow) in transverse section. Note high levels of expression of these peptide receptors in the cNA, a cranial motoneuron pool not related to respiration. Scale in

micrometers. cNA, compact formation of the nucleus ambiguus; scNA, subcompact formation of NA; rVRG, rostral ventral respiratory group; VII, facial motor nucleus; D, dorsal; L, lateral.

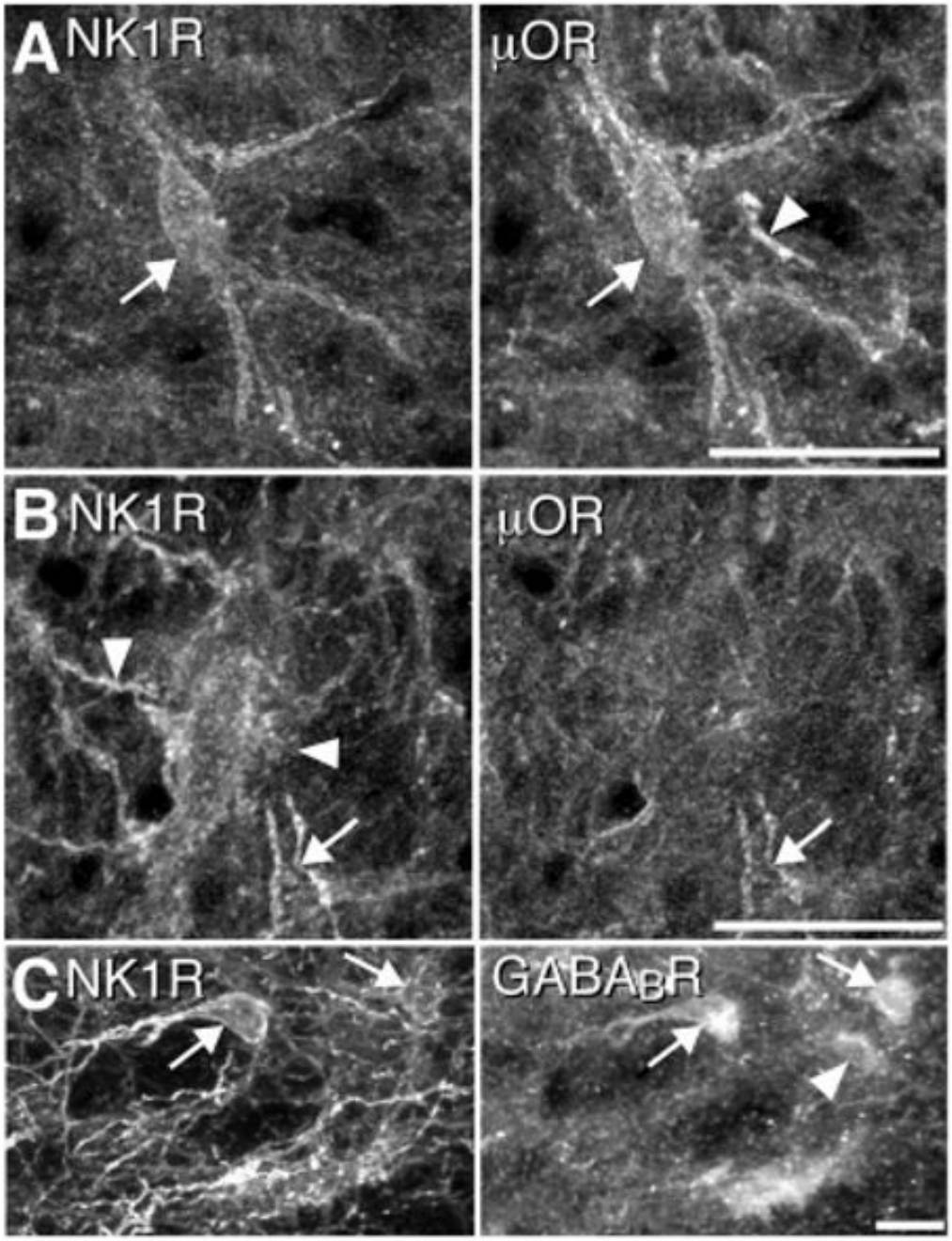

Fig. 3.

G-protein–coupled receptors are coexpressed on individual preBötC neurons. Confocal projections of NK1R$^+$ somas (**A** to **C**) (left) and processes (B) (left), μOR$^+$ somas (A) (right) and processes (A and B) (right), and GABA$_B$R$^+$ somas (C) (right). Arrows indicate coexpression and arrowheads indicate absence of coexpression. Bars = 25 μm.

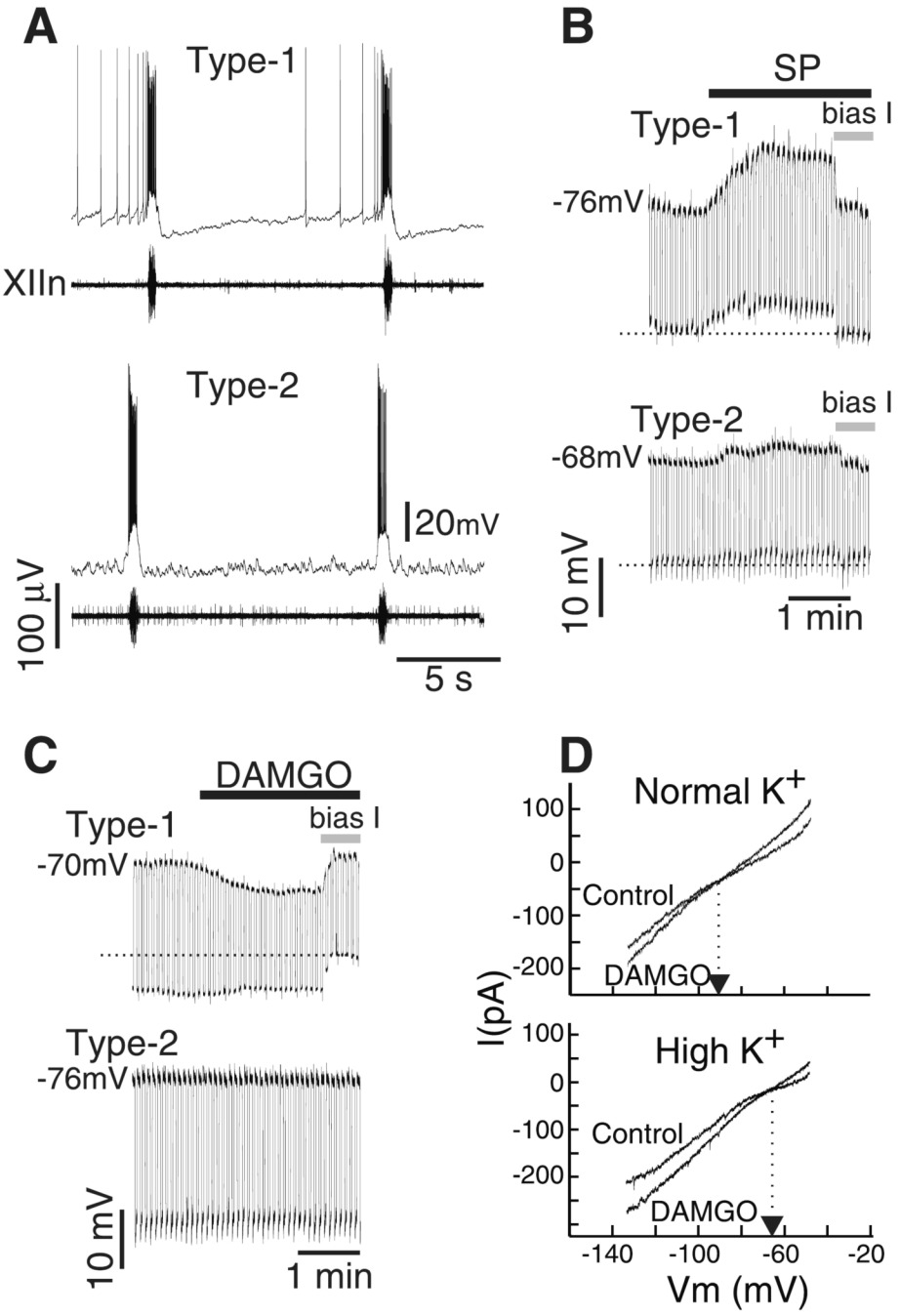

Fig. 4.

Postsynaptic membrane responses of inspiratory neurons in the preBötC to SP and DAMGO. (**A**) Characteristic membrane potential trajectory between inspiratory discharges of type 1 and type 2 inspiratory neurons. Note the long-lasting hyperpolarization characteristic of type 1 neurons. (**B**) Membrane responses of type 1 and type 2 neurons to bath-applied SP (1 µM) after blockade of action potential driven synaptic transmission by TTX (2 µM). Hyperpolarizing current pulses (1-s duration every 5 s) were injected to measure input resistance throughout the application and the membrane potential was brought back to control value by injecting bias current at the indicated time (bias I). (**C**) Membrane responses of type 1 and type 2 neurons to bath-applied 5 µM DAMGO (TTX). (**D**) (Top) *I-V* curves (in the presence of TTX) before and

after DAMGO application (5 μM) in normal $[K^+]_o$ (6.2 mM). Arrow indicates potential at which the two curves intersect. (Bottom) *I-V* curves (in the presence of TTX) before and after DAMGO application (5 μM) in high $[K^+]_o$ (16.2 mM). Note intersection points of the curves have shifted in the depolarizing direction.